SAND2008-2086C

Doppler Electron Velocimeter—Practical Considerations for a Useful Tool

Phillip L. Reu*
Sandia National Laboratories, PO Box 5800, Albuquerque, NM 87185

ABSTRACT
The Doppler electron velocimeter (DEV) is a potentially new dynamic measurement system for the nano-scale. Electron microscopes have been used for many years now for visualizing extremely small samples, but the ability to make dynamic measurements has not existed. The DEV proceeds along the analogous lines of a laser Doppler velocimeter, which uses the Doppler shift of the wave to detect the velocity. The use of electron beams with their extremely short wavelengths overcomes the diffraction limit of light of approximately ½-micron to measure samples of current scientific interest in the nano-regime. Previous work has shown that Doppler shifting of electrons is theoretically possible, this paper examines whether a practical instrument can be built given inherent limitations of using electron beams as a probe source. Potential issues and their solutions, including electron beam coherence and interference will be presented. If answers to these problems can be found, the invention of the Doppler electron velocimeter could yield a completely new measurement concept at atomistic scales.

Keywords: Nano, MEMS, vibrometry, dynamic measurements, electron microscopy

1. INTRODUCTION

Making dynamic measurements at the nano-scale will become increasingly important as areas of research as disparate as materials research to nano-machines are pursued. Microelectromechanical systems (MEMS) research has proven the need to know not just the quasistatic behavior of specimens, but their truly dynamic behavior is important as well. Building on the vast amount of work done to develop transmission electron microscopes (TEM), a Doppler electron velocimeter (DEV) is envisioned to open up this important field of nano-dynamics. This is assisted by the fact that analogs of nearly all of the traditional optical equipment are available including: coherent sources, beam-splitters, bi-prisms, lenses, imaging systems and detectors. These have been developed and optimized for situations other than for the DEV, so further development and modification of these will be required.

The theoretical background for the DEV has already been established [1], and this paper seeks to determine if it is experimentally practical. The key aspect to this is the answering the question: what are the measurement bandwidth limitations of the DEV? The answer to this question revolves around the joint issues of electron beam coherence and maximum available source current. These two questions are considered in light of realistic and existing electron microscope equipment including electron sources and detectors. These concerns, along with my preliminary answers, will be addressed. In addition, some ideas on experiments that may be conducted are outlined with example calculations to prompt discussion and ideas about potential applications for the DEV.

2. ELECTRON COHERENCE

2.1. Introduction to Electron Coherence

By definition, a coherent source is one which exhibits interference when two parts of the wave are overlapped via an interferometer. One must take care of how this interference is discussed as there is some basic confusion due to the counterintuitive nature of many quantum mechanical effects. For instance, in optics, the wave is typically described as being split at the beam-splitter and then recombined at some imaging device to create interference fringes. For electro-magnetic radiation such as light, this is likely an apt description because the photon of light is a boson. Bosons have the property of being able to be densely packed and are able to theoretically interfere with each other. This aids the experimentalist in allowing an extremely bright coherent source, the laser for instance, where at any given location in the beam-path, there are likely photons which can interfere. Electrons are fermions, which has two important limitations on interferometry. First, electrons can only interfere with themselves. This

* plreu@sandia.gov

means that to describe the interference the mathematics of the wave function must be used. The wave function, which represents the electron, is split by the beam-splitter and then recombined at a detector. What the detector "sees" is the magnitude of the wave function, or the probability that the electron will be at any given location at some point in time. This has the repercussion that electron holograms are built up by individual events accumulated over time to create the desired fringe pattern. This was most elegantly shown by Tonomura using an electron microscope [2,3], and described by Feynman [4]. The same effect of course can be observed with photons, but the possibility of having a large number of photons at any given location (i.e., high flux or irradiance) results in having "instantaneous" fringes. This density of photons, as defined in per cell of phase space in quantum mechanical terms is called the degeneracy. Even for photons with degeneracies of the order of 10^{12} [4], there is a practical limit on the rapidity of the fringe formation due to the power of the laser, but for most optical applications, this is typically not the limiting factor. For electrons, the degeneracy is limited to 1, in other words, two electrons of opposite spin per unit-cell of phase space [5-6]. This fundamentally limits the number of electrons per second from the source, or the brightness, B_{max}, to [7]:

$$B_{\max} = \frac{2e\Delta E}{h\lambda^2} \ (\mathrm{A\cdot cm^{-2}\cdot sr^{-1}}), \qquad (1)$$

where e is the electron charge, ΔE is the source energy spread, h is Plank's constant and λ is the electron wavelength. For a 300 keV electron and a degeneracy of 1, this leads to a maximum theoretical brightness of 3.9×10^{14} $\mathrm{A\cdot cm^{-2}\cdot sr^{-1}}$. Real sources have of course a lower brightness, typically in the range of 6×10^{9} $\mathrm{A\cdot cm^{-2}\cdot sr^{-1}}$.

This quantum mechanical assumption of fermion behavior is reinforced with the practical consideration that only one electron is traversing the interferometer at any given time. An electron spacing of 25 μm can be calculated by taking an electron beam with a current of 1 μA (a high current) and a velocity 1.6×10^{8} m/s (100 kV). This puts the spacing of the electrons at, much longer than the coherence length of 7 μm for an extremely monochromatic source, further confirming the single electron interference assumption. Once single electron interference is understood, it is easier to make some headway on understanding the concept of coherence in an electron interferometer.

Thinking about and explaining coherence and coherence limitations is often simplest in terms of Young's double slit experiment [8]. There are two inter-related types of coherence often termed transverse and longitudinal coherence. Both are illustrated in Figure 1 in relation to Young's double slit experiment. Transverse (or spatial coherence) is inversely related to the source size. That is, the smaller the source the greater is the transverse coherence. For interference to occur, the transverse coherence must be large enough to cover both holes of Young's interferometer. This is alternately described for larger non-ideal sources by taking the ideal point source and shifting it $\pm\varepsilon$, to represent the true source size. This is the same as saying the real source is a combination of ideal sources emitting independently of one another. Translating the ideal source has the physical effect of shifting the resulting fringes $\pm\Delta x$ as illustrated in the figure. If the translation of the fields is such that the shift is one fringe, the resulting fringe summation will average out the fringes and the source is said to be spatially incoherent. The longitudinal coherence is related to the source energy spread, i.e. how monochromatic is the source. The more monochromatic the source (smaller energy spread) the longer the temporal coherence. Each wavelength represented in Figure 1 by λ_1, $\lambda_2 \ldots \lambda_n$, creates a set of fringes of differing widths. The contributions of each of the wavelengths are again summed to yield a final fringe contrast. As can be imagined, if too broad a number of wavelengths contribute to the fringe formation, the contrast will decrease to zero. This physical description which imagines a single perfect source that can be varied in either wavelength or position is analogous to the more involved description of partial coherence introduced by Born and Wolf [9]. However for the DEV, as the source is only emitting one electron at a time from some location on the source, that emission by definition is a perfectly monochromatic point source. Furthermore, as the electrons only interfere with themselves, the concept of summing the resulting intensity patterns also makes intuitive sense.

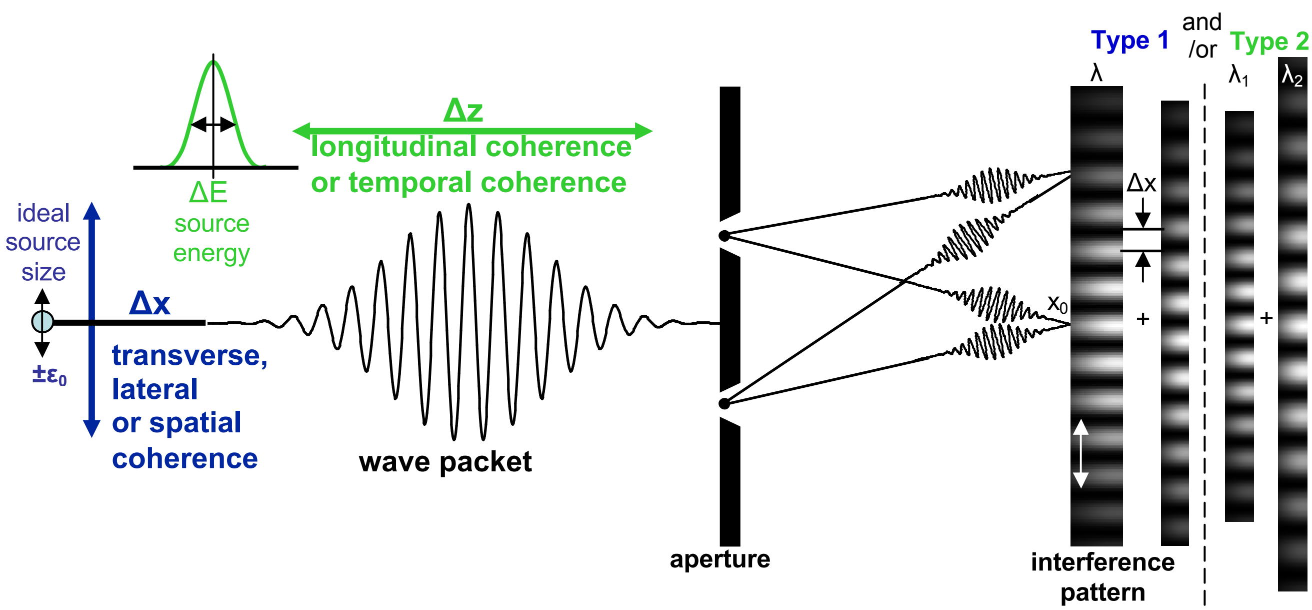

Figure 1. Young's double hole interferometer showing coherence effects on fringe contrast.

How does coherence affect the DEV? Longitudinal coherence is typically not a practical problem as sources with extremely small energy spreads are available (with some cost in beam current). Transverse coherence is generally considered more of an issue, not in that extremely small sources are not available, but the greater the transverse coherence required, the lower the resulting beam current. This current limitation directly influences the maximum fringe detection rate and therefore the bandwidth of the DEV. It is because of this current limitation that methods of circumventing the spatial coherence issues are being investigated.

To attempt to calculate a practical beam current, a derivation given by Lichte [10,11] that uses the van Cittert-Zernike theorem is useful. This theory is based on the idea that for nearly all sources, with the exception of lasers, the source can be viewed as an extended collection of independent radiators. Van Cittert-Zernike uses Fourier optical theory to transfer the coherence from the source to the image plane where interference takes place. The complete derivation is outlined by Lichte [10], and only briefly given here.

The source brightness, B, which is equivalent to that found in equation 1, but defined in terms of TEM characteristics is:

$$B = \frac{I}{A\Omega} \quad (\mathrm{A \cdot cm^{-2} \cdot sr^{-1}}). \tag{2}$$

Where the area of the source is $A=\pi r^2$, the solid angle may be expressed in terms of $\Omega=\pi\alpha^2$. Where r is the source size and α is the ½-angle illuminated by the source. Using these relations, the current can be expressed as:

$$I = B(\pi r\alpha)^2 . \tag{3}$$

This relation used with the van Cittert-Zernike theorem gives the coherent current as:

$$I(\mu) = \frac{-B\ln(\mu)}{k^2} , \tag{4}$$

where μ is the fringe contrast (or degree of coherence related to α) and k is the wave number. A quick discussion of these equations as they apply to Doppler measurements is in order. Equation 4 shows that the source brightness and the required fringe contrast are the two limitations to current. Unfortunately, the brightness is a fixed feature of the electron source and cannot be improved as discussed earlier. If α decreases, that is the source size is decreased, the spatial coherence (coherence area) increases as one would expect improving the fringe contrast μ. However, this in practice means limiting the aperture, which in turn limits the current, often severely. Fringe contrast can be sacrificed up to some extant, but that impacts the signal-to-noise ratio.

One possibility for improving the current is to find a method of reducing the coherence requirements. This would allow a larger aperture to be used and therefore a greater current. This has been shown to work in the optical domain with an arrangement often referred to as a Linnik microscope [12]. This traditional Michelson arrangement uses an LED as a light source for measuring out-of-plane motion of an object. The setup and optical arrangement of a Linnik system is more difficult, due to the requirement of matching the path length between the object and reference legs as well as aligning the image from both legs. Figure 2 shows this pictorially with the microscope in imaging mode. The easiest way to visualize how this works is by thinking of the source as having areas of coherence, that if aligned will interfere. This is not unlike a speckle pattern in digital speckle pattern interferometry (DSPI). Using this setup, Doppler signals have been obtained. To increase the signal at the detector, the source was focused onto the object and reference and then aligned onto a single point detector with the result of increased Doppler signal. This implies via analogy, that a less or even incoherent source could potentially be used for obtaining Doppler signals with an electron microscope. The importance of this conclusion is that greater current is available at the detector, which in turn increases the bandwidth of the detector. This opens the possibility of utilizing a greater portion of the emitted electron current.

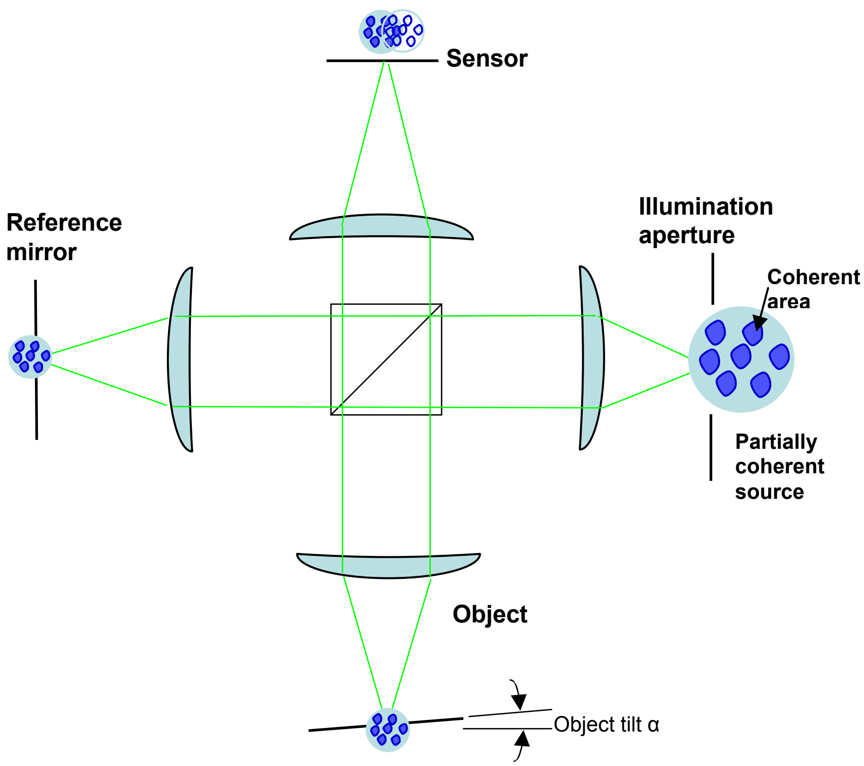

Figure 2. Linnik microscope alignment with incoherent source.

2.2. Practical beam currents and what they mean for detection

It is useful to consider what the detector will see during a measurement. The moving fringes will appear as a time varying intensity. To make a successful measurement, there needs to be enough current for a detector to measure. So what are some practical beam currents? I will give a range of values based on various assumptions. First, starting with the maximum theoretical brightness, and using some realistic numbers for beam semi-angle and source size, a beam current of milliamps can be calculated—this is certainly much higher than can be currently obtained. Using currently available source information, a more realistic current of 85 nA can likely be achieved [7]. Voelkl quotes a value for holography of 2-5 nA [13]. It is obvious that the greater the current the higher the possible bandwidth of the DEV. For the next section discussing possible experiments, a conservative estimate of a beam current of 1 nA will be assumed that with current sensing technologies would lead to a detection bandwidth of approximately 1 MHz.

3. POSSIBLE EXPERIMENTS FOR THE DOPPLER ELECTRON VELOCIMETER

One of the powers of the DEV is that the electron beam, unlike a laser, can be affected by not just the velocity of a surface as in a traditional laser Doppler application, but by a varying magnetic or electric field. Really, anything that changes the phase of the passing electron beam can be a candidate for DEV measurements. This is seen in the following equation given without derivation [13]:

$$\Delta\varphi = \frac{1}{\hbar}\oint(m\mathbf{v} - e\mathbf{A})d\mathbf{S}\ . \qquad (5)$$

where φ is the phase, $\mathbf{v}$ is the velocity, $\mathbf{A}$ is the electromagnetic field vector potential, $\mathbf{S}$ is the integration path containing the area between the object and reference beam and $\hbar$ is Plank's constant divided by 2π. This is an important equation and somewhat difficult to understand. It states that the wavefront is not perpendicular to the direction of moment, $m\mathbf{v}$, as is typically the case, but is perpendicular to the generalized momentum ($m\mathbf{v}$ - $e\mathbf{A}$), often termed the canonical momentum. Equation 5 leads to an ambiguity in the phase calculated when an electron travels through an electromagnetic field because the vector $\mathbf{A}$ is not uniquely defined. This is overcome practically by integrating around a closed loop that contains the object beam and the reference beam. The magnetic or electric fields referred to are those contained between the two beams of the interferometer. Equation 5 can be simplified with some further math and separated into an electrostatic and magnetic portion:

$$\Delta\varphi = \frac{e}{\hbar}\int mv^2 dt - \frac{e}{\hbar}\int \mathbf{B}d\mathbf{S} = \frac{eLU}{\hbar v} - \frac{e}{\hbar}\oint \mathbf{B}d\mathbf{S}\ . \qquad (6)$$

where $\mathbf{B}$ is the magnetic field, U is the electric field, and L is the distance traveled through the field. The first portion of the equation is the effect of the electric field on the phase and the second contains the effect of the magnetic field. This equation does not, however, include the energy shift due to inelastic scattering off of a moving surface which is the first topic I will address.

3.1. Mechanical motion

Mechanical motion of an object is the first type of motion traditionally associated with Doppler. In an electron microscope it works by setting up a beam splitting interferometer and reflecting a portion of the beam onto the sample, which reflects it back to be recombined to create the moving fringes. The object in this arrangement is functioning as an electron mirror. An electron mirror can be created if the surface of the object is conducting, and held at a potential. In front of the mirror is another electrode which causes the electrons to reverse direction after reaching the surface of the object. With the DEV setup in this configuration, the resulting Doppler frequency is:

$$f_D = \frac{d\varphi}{dt} = \frac{4\Delta v}{3\lambda}, \qquad (7)$$

where f_D is the Doppler frequency in Hz, dφ/dt is the instantaneous rate of phase change, Δv is the velocity difference between the object and reference leg of the interferometer. Using this relation and varying the electron energy, an idea of the range of velocities able to be measured can be determined as shown in Table 1.

3.2. Varying electric field measurements

The electric field applies a force to the passing electrons which changes the phase of the reference leg in relation to the object leg according to Equation 6. This arrangement has been used typically to measure either a samples thickness or its mean inner potential. Other examples have used the phase shift to measure the coherence length of an electron beam by changing the applied field until loss of fringe contrast occurs indicating a phase shift greater than the coherence length has occurred [14]. Of course, if the electric field is time-varying, a time varying phase shift, or Doppler frequency will result according to the following equation:

$$f_D = \frac{d(\Delta\varphi)}{dt} = \frac{eL}{\hbar v}\frac{dU}{dt}, \qquad (8)$$

where U is the potential difference between the object and reference beams, v is the group velocity and L is the distance the beam travels through the electric field. Table 1 shows the measurable field changes in kV/s for a 1 MHz bandwidth DEV. Because the Doppler frequency depends on the velocity of the electron through the field, the sensitivity of the DEV can be varied by changing the electron velocity, controlled by the accelerating potential of the microscope. That is, by using a low energy electron beam (slow electrons) greater sensitivity to the electric field is obtained.

3.3. Varying magnetic field measurements

Another quantity that can be measured is the magnetic field. This property has already been exploited in electron holography to measure static and quasi-static magnetic fields in various materials [2]. The equation simplified from above relates the magnetic field to the Doppler frequency by:

$$f_D = \frac{d(\Delta\varphi)}{dt} = \frac{eL}{\hbar}\frac{d\Phi_m}{dt}, \qquad (9)$$

where $d\Phi_m/dt$ is the time varying rate of the magnetic field change in Webers/s contained between the object and reference beams. Interestingly, the phase change only depends on the path and the magnetic flux and is not related to the electron beam energy.

Table 1. Dynamic rates for a 1 MHz sampling capability.

TEM Parameters			Measured Properties		
Source Acc. (kV or keV)	electron λ (nm)	electron v (m/s)	v (μm/s)	dU/dt (kV/s)	dφ/dt (Wb/s)
0.01	0.38783	1.88E+06	290.87	1	6.58E-10
0.1	0.12264	5.93E+06	91.98	4	6.58E-10
10	0.01220	5.85E+07	9.15	38	6.58E-10
100	0.00370	1.64E+08	2.78	108	6.58E-10
200	0.00251	2.08E+08	1.88	137	6.58E-10
1000	0.00087	2.82E+08	0.65	186	6.58E-10

4. CONCLUSIONS

This paper briefly outlines the parameters required for a practical DEV. The two most important are the beam current and related to this the coherence of the electron beam. Practical limits on beam current for existing sources places the maximum at a few nA for a fully coherent source. This will likely need to be increased to make a useful device, but there appears to be room to do this. The most likely approach to increase the current will be to loosen the coherence requirements. This has been shown to be successful with the optical analogy to the Linnik microscope. Even with the limits on current equipment, Table 1 shows a range of velocity, magnetic and electrostatic field rates which could be measured with existing equipment. Most likely the first practical experiments are magnetic field measurements where a number of experiments have already been conducted at video rates, and there is a definite need for greater rates that would fall within the sensitivity and bandwidth of the DEV.

ACKNOWLEDGEMENTS

I would like to thank Bruce Hansche for conducting optical analog experiments which have confirmed some suspicions, as well as many fruitful discussions helping me sort out my thoughts. Sandia is a multiprogram laboratory operated by Sandia Corporation, a Lockheed Martin Company, for the United States Department of Energy under contract DE-AC04-94AL85000.

REFERENCES

1. Reu, P.L., “Doppler Electron Velocimeter—a Proposed Nano-scale Dynamic Measurement System,” Proceedings of the Society for Experimental Mechanics, Springfield, MA 2007.
2. Tonomura, A., *Electron Holography 2nd edition*, Springer, New York, 1999.
3. For a great movie of this experiment see – http://www.hqrd.hitachi.co.jp/em/movie.cfm
4. Feynman, R.P., Leighton, R.B., Sands, M., *The Feynman Lectures on Physics*, Addison-Wesley Publishing Co., Menlo Park, CA, 1977.
5. Silverman, M.P. “On the feasibility of observing electron antibunching in a field-emission beam,” Physics Letters A, **120**, 442-446 (1987).
6. Spence, J.C.H., Qian, W., Silverman, M.P., “Electron source brightness and degeneracy from Fresnel fringes in field emission point projection microscopy,” J. Vac. Sci. Technolo. A, **12**, 542 (1994).
7. Spence, J.C.H., Howells, M.R., “Synchrotron soft X-ray and field-emission electron sources: a comparison,” Ultramicroscopy, **93**, 213-222 (2002).
8. Young, T. . Philos. Trans. R. Soc. XCII 12 (1802) 387; Young’s works, Vol. 1, pp. 140, 170.
9. Born, M., Wolf, E., *Principles of Optics*, Cambridge University Press, 1999.
10. H. Lichte, *Advances in Optical and Electron Microscopy*, Academic Press **12** (1991) p. 45.

11. H. Lichte, “Performance limits of electron holography,” Ultramicroscopy, (2007) to be published.
12. Abdulhalim, I., “Competence between spatial and temporal coherence in full field optical coherence tomography and interference microscopy,” J. Opt. A: Pure Appl. Opt. **8** (2006) 952–958.
13. Voelkl, E., Allard, L., Joy, D., *Introduction to Electron Holography*, Kluwer Academic, New York, 1999, p. 61.
14. Schmid, H., “Coherence Length Measurement by Producing Extremely High Phase Shifts,” Proceedings of the European Conference on Electron Microscopy, Budapest, 1984.

15. Gabor, D., “Light and Information,” Progress in Optics, **1**, 147 (1961).
16. Spence, J.C.H., W. Qian, M.P. Silverman, “Electron source brightness and degeneracy from Fresnel fringes in field emission point projection microscopy,” J. Vac. Sci. Techn. A, **12**, 542 (1994).
17. Tonomura, A., *Electron Holography*, Springer (1999) p. 18.
18. M. Born and E. Wolf, *Principles of Optics*, Cambridge University Press (1999) p. 572.
19. J. Goodman, *Statistical Optics*, John Wiley and Sons (2000) p. 207.
20. Linnik paper
21. L. Marton, “Electron Interferometer,” Physical Review, **85** (1952) 1057.
22. G. Matteucci and G. Pozzi, “A “mixed” type electron interferometer,” Ultramicroscopy **5** (1980) 219.
23. R.A. Herring, G. Pozzi, T. Tanji, A. Tonomura, “Interferometry using convergent electron diffracted beams plus an electron biprism (CBED + EBI),” Ultramicroscopy **60** (1995) 153.